The EAST protein of *Drosophila* controls an expandable nuclear endoskeleton

Martin Wasser and William Chia

Institute of Molecular and Cell Biology, National University of Singapore, 30 Medical Drive, Singapore 117609
e-mail: mcbwchia@imcb.nus.edu.sg

The high degree of structural order inside the nucleus suggests the existence of an internal nucleoskeleton. Our studies on the *east* gene of *Drosophila*, using the larval salivary gland polytene nucleus as a model, demonstrate the involvement of an extrachromosomal nuclear structure in modulating nuclear architecture. EAST, a novel ubiquitous protein, the product of the *east* (*enhanced adult sensory threshold*) locus, is localized to an extrachromosomal domain of the nucleus. Nuclear levels of EAST are increased in response to heat shock. Increase in nuclear EAST, whether caused by heat shock or by transgenic overexpression, results in the expansion of the extrachromosomal domain labelled by EAST, with a concomitant increase in the spacing between chromosomes. Moreover, EAST functions to promote the preferential accumulation of the proteins CP60 and actin in extrachromosomal regions of the nucleus. We propose that EAST mediates the assembly of an expandable nuclear endoskeleton which, through alterations of its volume, can modulate the spatial arrangement of chromosomes.

The high degree of structural organization of the cell nucleus is well documented. Interphase chromosomes are partitioned into distinct chromosome territories[1] and often show a polarized orientation[2]. Enzyme complexes engaged in genomic functions such as replication, transcription and pre-mRNA metabolism cluster to form higher order domains rather than being diffusely distributed throughout the nucleus[3-6]. Measurements of chromatin motion *in vivo* suggest that chromosomes undergo diffusional movements, which are confined to a subregion of the nucleus[7,8]. However, the organizing principle of structural order within the nucleus is poorly understood.

A nucleoskeleton might have a role in the structural organization of the nucleus by providing anchorage for macromolecules and imposing a restraint on their mobility. A major component of the nucleoskeleton is the lamina, a meshwork of intermediate filaments on the inner surface of the nuclear envelope that has the ability to interact with chromatin[9,10]. In contrast to this well-characterized nuclear shell or exoskeleton, however, the existence of a nuclear endoskeleton remains a matter of debate. The nuclear matrix, an operational definition referring essentially to the non-chromatin fraction of the nucleus[11], has been postulated to harbour an internal non-chromatin backbone of the nucleus[12]. Candidate proteins, which may serve as building blocks of a possibly filamentous nuclear endoskeleton have not yet been identified, however. Some models predict the involvement of actin, which has been detected both in nuclear matrix fractions[13] and by immunofluorescence studies in the nucleoplasm of dinoflagellates[14] and mice[15].

A likely site of a nuclear endoskeleton would be the proposed interchromosomal domain compartment that separates chromosome territories[16]. An analogous structure was visualized in *Drosophila* polytene nuclei by *in situ* hybridization of nuclear RNA and termed the extrachromosomal channel network[17]. This nuclear network has also been shown to be labelled by the *Drosophila* Tpr protein[18]. An interchromosomal nuclear compartment could also be visualized in diploid human cells by polymerized nuclear-targeted vimentin[19], indicating that such a structure is not restricted to giant polyploid insect nuclei.

In this study, we used the *Drosophila* giant polyploid nuclei of larval salivary glands and the diploid nuclei of germ cells as models to investigate the role of the EAST protein in nuclear architecture. We show that EAST is a component of an expandable extrachromosomal nuclear domain in Drosophila nuclei that we will refer to as the extrachromosomal nuclear domain (END). The level of EAST dramatically influences the relative volume of the END. An increase in nuclear EAST leads to an enlargement of this extrachromosomal structure, resulting in concomitant changes in the spacing of chromosomes. Our results support a model in which EAST regulates a dynamic nuclear endoskeleton that can recruit other nuclear proteins and modulate the spatial configuration of chromosomes.

Results

***east* encodes a novel non-chromosomal nuclear protein.** The *east* (*enhanced adult sensory threshold*) gene of *Drosophila* has been described previously[20,21]. The gene has been identified in an insertional mutagenesis screen as a viable P-element insertion allele (Fig. 1a). Mobilization of the transposon allowed the generation of a series of lethal deletion alleles with different lethal phases, indicating that the *east* gene is essential for viability (Fig. 1a). Genomic and complementary DNA clones corresponding to the *east* locus were isolated. The longest cDNA clone obtained was 6.3 kilobases (kb). Using 5′RACE, a full-length cDNA sequence of 7,349 base pairs (bp) was assembled. Sequence comparisons of the plasmid rescued genomic DNA and five independent RACE clones with identical 5′ ends revealed that the P element was integrated 183 bp upstream of the putative transcription start of the *east* gene. On Northern blots, the *east* cDNA detected two related mRNA species of ~8 kb and 10 kb (data not shown) as previously described[21]. Genomic probes extending as far as 10 kb upstream of the putative transcriptional start site failed to identify additional transcripts.

The *east* cDNA encodes a novel predicted translation product of 2,362 amino acids (Fig. 1b) with a predicted relative molecular mass (M_r) of 253,000 (253K), henceforth referred to as EAST. The program PSORT II (ref. 22) detected seven sites containing potential nuclear localization sequences (NLS), three of the bipartite type and six of the monopartite type. The program PESTfind[23] was used for the prediction of potential PEST regions, which target proteins for rapid degradation. Most PEST sequences proven to function as proteolytic signals have scores greater than +5. Twelve potential PEST sites were detected within EAST, with PEST scores ranging from +5.8 to +19.2. No other motifs could be found within the EAST sequence. The sequence analysis therefore suggested that EAST might be an unstable protein targeted to the nucleus.

To study the expression pattern and subcellular localization of EAST, four non-overlapping portions of the *east* cDNA were expressed as hexahistidine (His_6) fusion proteins in *Escherichia coli* and used to raise polyclonal antibodies (see Methods). The four distinct antisera gave identical staining profiles, labelling nuclei of all

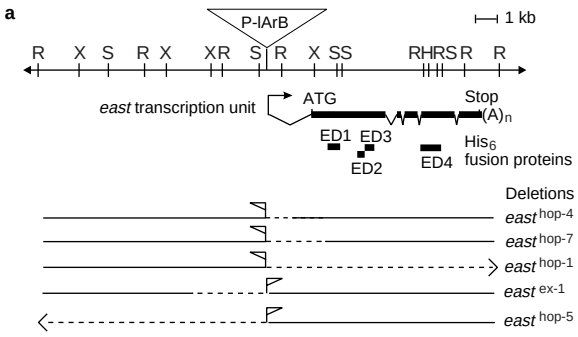

b

```
   1 MGPNHCDSNWTQSASDRREQQEVVEQQARRRRGSGHHRSSNVGSSSQGPS
  51 RMSSRKVPGGSGGADESTAATAPLDDNANASVEIPASSEEPAMGVGEEMS
 101 IISKTRTSTLSVEPAKEPTVTAELEGEKELESNPVSKTPRSTPTPTLTPA
 151 VTPTASDGVAAKSVRVTRHSSPLLQIISPTTSRREVGDGELDTEEPTGSG
 201 GQRKKSSVERSLAPVIRGRKSIKDLKEAKEVKSEEPPAAASESRAASGVTP
 251 GQVKEQHDADGNEMESLPITDKKDHKDTKDKGDERETNQEEEKEKSADTE
 301 IIADTEKTSEKQKYTEKDKAADKDGGKEKDIDANKDIDKEKEKVKEVLPP
 351 VVPIAPVTPTCNRVTRKFTLPRSRRLTTRVTSQFVASPLPVGANSTASLV
 401 AASSSVTEQPPPSRGRRKKPVVVAPPLEPAVKRKRSQDVEADSDANNSTK
 451 YSKVEVVKSEEAEAPEEDSSAVPIKQESVDGNEVSSISPTVTPTPTPAPT
 501 PAPVPGSRRGRGRPQNRNSSSPATTTRATRLSKAGSPVILTPVAQEPAPP
 551 KRRRVCSSTRKTVSASSLAPSSQGGAGDEDSKDSMASSMDDLLMAAADIK
 601 QEKLTPDFDDSLMPEGLPSTSGASSANGHSCTEPLTVDTEINVKPADSKV
 651 KPKESPVVAVEESPSQSETQSAKVSAHAGKAPSLSPDMISEGVSAVSVRK
 701 FYKKPEFLENNLGIEKDPELGEIVQTVSNNDTETDVEMAVDGEVNQPSTP
 751 KSQDKKKEEQEKNQKSGLKAAKKAPAKLEPKAEDISEILTDVPVDISTEA
 801 VEIIEEAEEDTCSNSSIKPGELRLDESNDEPELLLEDALIVNGDENETPD
 851 QPEEKEDQVEFFHTGEYDDFEHEIMVELAKEGVLDASGNALSQQKVELEH
 901 PEDVTLHESKNDIEAEESVERKPLKDPSVADEMEDMNEESYIDIKDQTNQ
 951 LLVEHLGRRGHGSDCGPEDNKKNLSTSASSTAADGLDIQLAIKEDDDEEK
1001 PLAVIADEQKPGLLLTNDMKVDEKPNGKQESVCDEHVQLVPNLRQEQEIH
1051 LQNLGLLTHQAAEHRRKCLLEAQARQAQMQLQQHHHHQHKRQGARGGGSA
1101 THVESSGTLKTVIKLNRSSNGGVSGSGGLPTGTVIHGGCGSSSASSTSSS
1151 SVGSATRKSSGTLGSGAGAGAGVRRQSLKMTFQKGRARGHGAADRSADQY
1201 GAHAEDSYYTIQNENEDSSHSESQSQTDHGFYQMVKKDEKEKILIPEKAS
1251 SFKFHPGRLCEDQCYYCSGKFGLYDTPCHVGQIKSVERQQKILANEEKLT
1301 VDNCLCDACFRHVDRRANVPSYKKRLSASGHLEMGSAAGSALEKQFAGDS
1351 GVITESGGEAGSTAAVAVQQRSCGVKDCVEAARHSLRRKCIRKRVKKYQL
1401 SLEIPAGSSNVGLCEAHYNTVIQFSGCVLCKRRLGKNHMYNITTQDTIRL
1451 EKALSEMGIPVQLGMGTAVCKLCRYFANLLIKPPDSTKAQKAEFVKNYRK
1501 RLLKVHNLQDGCHELSEADEEEAPNATETERPTSDGHEDPEMPMVADYDG
1551 PTDSNSSSSSTAALDTSKQMSKLQAILQQNVGADAAGAAGTGTVAASPGE
1601 ADLGQISLTYCEGIRTFPCANFSTARKSWVCSSRCRSDAAAASVLRRAGH
1651 ECRLSYNTMSRRAASGRSCKSRTKSELISAPVDTIREVLPKRRSRPSTHA
1701 SSNASVYTETVRQRLNSFDHGHCGGLNIAGSPSSSGSGKRSGVPQPTGAS
1751 VLATALTTPLTSHSSSSASISSEQHSSVDPVIPLVDLNDDDEGEDGAGGA
1801 GERESTNRQQDVILECLRTASVDKLTKQLSSNAVTIIARPKDKSQLSCNS
1851 GSSTSISSSSSAISSPEKWPSLRLQQSHQSSPRMHRHWPPASSGVSNSRS
1901 ILKTNLLGMNKAVELVPLTTAPHAYKPTGCHKPEKQQKILDVANKQPGSQ
1951 GEPVPSSALLGLQSKLKPPTHQQQVSGSGAGTSGSQKPSNVAQLLSSPPE
2001 LISLHRRQTSGAAAGSSSFLQGKRLQLPRSGAGPSGAGTGTGAGAAGSRS
2051 AGGPPPPNVVILPDALTPQERHESKSWKPTLIPLEDQHKVPNKSHALYQT
2101 ADGRRLPALVQVQSGGKPYLISIFDYNRMCILRREKLMRDQLLKSNAKPK
2151 PQNQQQQQGQTHQQQQNSAACAAFSNMVKLAQQHTARQQLQQLQQKPQQQ
2201 QQLPTLQPGGVRLARLPQKLLMPPLTNPQIGSQAPNLQPLLSSTLDNSNN
2251 CWLWKNFPDPNQYLLNGNGGGAGSSSSKLPHLTAKPATATSSSGAANKSA
2301 GSLFTLKQQQHQQKLIDNAIMSKIPKSLTVIPQQMGGNTGGDMGGSSSPA
2351 RTDDGEGGRHGH
```

Figure 1 **Genomic organization of east and the sequence of the EAST protein.** **a**, The restriction map of the *east* locus is aligned with a graphical representation of the transcription unit corresponding to the polyadenylated *east* cDNA of 7.3 kb. The P element P-lArB is inserted 183 bp upstream of the putative transcription start site (arrow). The start codon (ATG) is located in the second exon. Thick lines indicate exons and the gaps in between, known introns. The positions of the cDNA fragments expressed as His_6 fusion proteins (ED1–4) are shown below. Dotted lines indicate the deletions associated with the lethal alleles $east^{hop\text{-}4}$, $east^{hop\text{-}7}$, $east^{hop\text{-}1}$, $east^{ex\text{-}1}$ and $east^{hop\text{-}5}$, resulting from the mobilization of the P element. The alleles $east^{hop\text{-}4}$ and $east^{hop\text{-}7}$ that die as late pupae and do not produce detectable EAST in larvae were used in our study. H, *Hin*dIII; R, *Eco*RI; S, *Sal*I; X, *Xho*I. **b**, The transcribed region of the *east* gene contains an open reading frame of 2,362 amino acids. Putative nuclear localization sequences (NLS) (white letters), bipartite NLS (italics) and potential PEST regions (bold letters) are shown. Superscripts indicate the flanking basic residues of each PEST region.

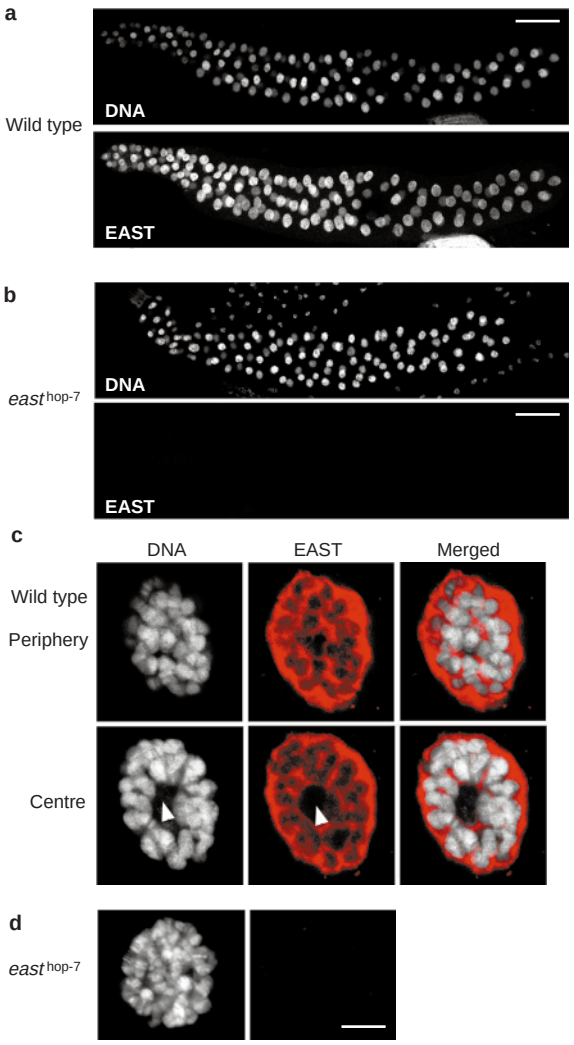

Figure 2 **Nuclear and extrachromosomal localization of EAST.** The *east* gene encodes a ubiquitous nuclear protein. **a**, The anti-EAST antibody (bottom panel) stains all nuclei of a third-instar larval salivary gland visualized by DNA staining (top panel). **b**, No specific EAST labelling could be detected in $east^{hop\text{-}7}$ mutant larvae. **c**, In larval salivary glands, EAST (red) is distributed throughout the extrachromosomal space of nuclear interior and periphery in a meshwork pattern. The giant chromosomes are shown in white. Optical sections through the periphery (top panels) and centre (bottom panels) of the same nucleus are shown. Note that EAST is excluded from the central nucleolar domain devoid of DNA (arrowhead). **d**, No anti-EAST labelling was detected in $east^{hop\text{-}7}$ salivary gland nuclei. Scale bars represent 100 μm (**a**,**b**) and 10 mm (**c**,**d**).

cell types in all developmental stages analysed, and thus indicated that EAST is ubiquitously expressed (Fig. 2a). These antibodies also either failed to detect or detected drastically reduced levels of protein in late embryos and larvae hemizygous for several lethal alleles of *east* including the deletion alleles $east^{hop\text{-}4}$ and $east^{hop\text{-}7}$ (Figs 1a and 2b), confirming that the *east* gene produces the nuclear antigen.

To gain insight into the subnuclear distribution of EAST, antibody stainings were performed on the giant nuclei of larval salivary glands, a convenient model for cytological studies. Polytene chromosome arms can be easily visualized and the chromosomes retain the arrangement they adopt in diploid interphase nuclei[24]. In these polytene nuclei, anti-EAST antibodies label the peripheral and interior extrachromosomal space in a meshwork-like pattern (Fig. 2c). The antibody labelling does not co-localize with chromosomes and

is excluded from a large central domain devoid of DNA staining, occupied by the nucleolus. Fixed squashes of salivary gland polytene chromosomes were not stained (data not shown), supporting the conclusion that the immunoreactivity is not associated with chromosomes. We will refer to the nuclear domain labelled by the anti-EAST antibody as the extrachromosomal nuclear domain (END).

EAST is a component of an expandable nuclear domain. The levels of nuclear EAST could be increased by heat shock. When feeding wild-type third-instar larvae were subjected to heat shock at 37 °C for 1 hour, a variety of larval tissues, including salivary glands and imaginal discs, showed a drastically enhanced anti-EAST labelling compared to non-heat-shocked controls (Fig. 3a–d). The transient accumulation of EAST induced by heat shock was accompanied by an expansion of the END. The normally fibrous anti-EAST staining pattern (Fig. 3c) changed to a more contiguous distribution, interrupted by channel-like exclusions that were occupied by chromosomes (Fig. 3d). DNA staining of polytene nuclei revealed that the arrangement of chromosomes shifted from a densely packed to a more open configuration, with wider gaps separating the chromosomal arms. The change in the spacing between chromosomes could also be observed in vivo in a transgenic line expressing histone 2A tagged with green fluorescent protein (His-GFP)[25], ruling out the possibility that this phenotype resulted from a fixation artefact (Fig. 3g). The coincidence of chromosomal rearrangements and increased nuclear EAST in response to heat shock suggested that the swelling of the END might help to push the chromosomes apart. In summary, heat shock can lead to an enlargement of the nuclear domain labelled by EAST.

EAST is required for the correct targeting of CP60 within the nucleus. On the basis of its subnuclear distribution, EAST might be a component of a flexible nucleoskeleton. If EAST were involved in forming a structural backbone, loss of *east* function might prevent other factors from being localized to the extrachromosomal region. The analysis of the CP60 protein provided evidence for this model. CP60 is a *Drosophila* protein that shuttles between the centrosomes and the nucleus in a cell-cycle-dependent manner[26]. In embryonic nuclei, CP60 is localized to a fibrous nuclear structure, which does not overlap with DNA or the nucleolus[27]. In nuclei of larval salivary glands, CP60 was found in two distribution patterns that could be seen simultaneously in the same gland. One appears fibrous and network-like, and essentially co-localizes with EAST protein (Fig. 3c). The other is characterized by several prominent spots that are found within the END and outside of the chromosomes (data not shown). Upon heat shock, CP60 distribution is modulated similarly to that of EAST, leading to an expansion of interchromosomal CP60 staining, which shows a high degree of co-localization with EAST (Fig. 3d). This suggests that both EAST and CP60 are likely to be components of the same expandable interchromosomal nuclear domain.

The loss of *east* function also affects the subnuclear distribution of CP60. In two *east* mutants $east^{hop\text{-}4}$ and $easthop^{-7}$, which do not produce detectable EAST protein in larval tissues (Fig. 2d), CP60 was still nuclear, showing that nuclear import of CP60 does not depend on EAST. In the absence of EAST, however, CP60 does not show a distinct network-like extrachromosomal distribution. Compared with wild type (Fig. 3c), the overall labelling pattern appeared more diffuse (Fig. 3e). To test if EAST was involved in targeting additional CP60 to the extrachromosomal region during heat shock, larvae of the two mutant *east* alleles were subjected to the heat-shock conditions described above. As expected, even after heat shock, EAST could not be detected in any larval nuclei (Fig. 3f). In the absence of EAST, CP60 failed to accumulate preferentially in the extrachromosomal space. Instead, it was distributed in a more random pattern that partially overlapped with DNA staining (compare magnifications of Fig. 3d, f). Similar differences in distribution of CP60 between wild-type and *east* mutants were seen in the polytene nuclei of the proventriculus (data not shown). These results show

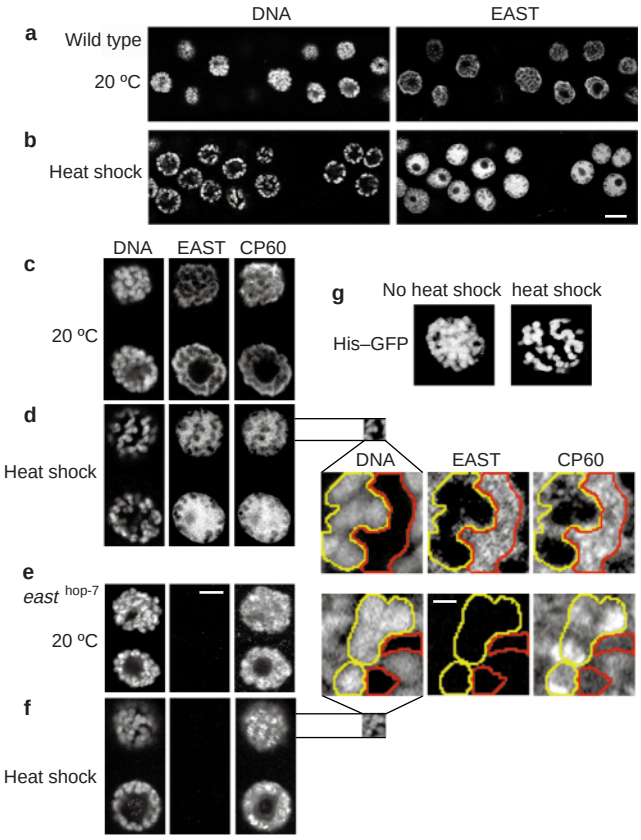

Figure 3 **EAST is a component of an expandable nuclear domain that also contains CP60.** Salivary glands of wild-type (**a–d**) and mutant $east^{hop\text{-}7}$ (**e, f**) feeding third-instar larvae raised at 20 °C. Larvae in (**b, d, f**) were subjected to a 1-h heat shock at 37 °C before analysis. Fixed larval tissues were triple labelled using DNA stain, anti-EAST and anti-CP60. **a, b**, Low-magnification views showing fields of wild-type salivary gland nuclei. Note the difference in the levels of EAST as well as the appearance of the DNA staining between the non-heat-shocked (**a**) and heat-shocked (**b**) glands. **c–f**, Higher-magnification images of two adjacent nuclei each, with a peripheral section shown for the top nucleus and a more central optical section shown for the bottom nucleus in each panel. Heat shock causes an expansion of the extrachromosomal space labelled by EAST and a wider spacing between chromosome strands (compare **c** and **d**). The extrachromosomal region is also labelled by CP60, which co-localizes with EAST. **e**, In the absence of EAST protein, CP60 shows a more diffuse distribution than in wild type. When $east^{hop\text{-}7}$ larvae were heat shocked (**f**), we could not observe as pronounced an increase in spacing between chromosomes as in wild type. Magnifications of boxed sections in heat-shocked wild-type (**d**) and *east* mutant (**f**) nuclei demonstrate that the correct targeting of CP60 to the extrachromosomal space depends on *east* function. Yellow lines drawn around the chromosomal territories and red lines drawn around extrachromosomal spaces were projected onto the anti-EAST and anti-CP60 stainings. In wild-type (**d**), EAST and CP60 predominantly accumulate in extrachromosomal regions. In the absence of EAST (**f**), CP60 shows a converse distribution pattern. Patches of CP60 labelling overlap with chromosomal territories where the labelling intensity is often higher than in adjacent extrachromosomal territories. **g**, The increased spacing between chromosomes that is induced by heat shock could also be observed *in vivo* using GFP-tagged histone (His-GFP) as a marker for DNA. Compare a nucleus of a larva exposed to 37 °C for 1 h (right panel) with nucleus from a non-heat-shocked counterpart (left panel). Scale bars represent 20 μm (**a,b**); 10 μm (**c-f**); and 2 μm (expanded inserts from **d** and **f**).

that EAST is required to recruit CP60 to an expandable, extrachromosomal structure of the nucleus.

Overproduction of EAST leads to an enlargement of the extrachromosomal space in the nucleus. As described above, heat shock

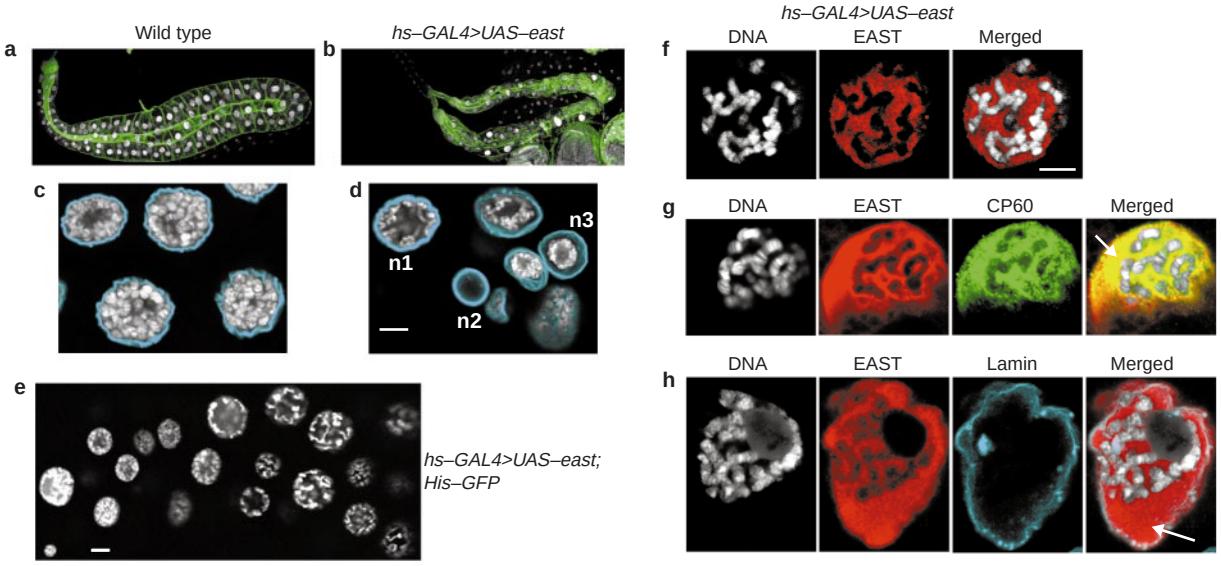

Figure 4 **Overexpression of EAST leads to an expansion of the END.** Salivary glands of third instar wild-type larvae (**a, c**) and third instar transgenic east-overexpressing larvae (**b, d–h**). Overexpression of EAST leads to retardation of the development of salivary glands. Compare the size of wild-type (**a**) and *UAS-east*; *hs-GAL4* (**b**) glands labelled with a DNA dye (white) and phalloidin (green) to visualize the outline of cells. Note the variability of the DNA staining compared with wild type. Double staining of wild-type (**c**) and transgenic (**d**) polytene nuclei using a DNA dye (white) and anti-nuclear lamin (cyan) to visualize the nuclear envelope. Prolonged overexpression produces high variability in nuclear diameter, DNA content (compare n1 and n2) and configuration of chromosomes, which can adopt a relaxed (n1) or compressed (n3) configuration. Also note the pronounced gap between chromosomes and nuclear envelope in n3. **e**, The hallmark phenotypes resulting from strong *east* overexpression in salivary glands could also be observed *in vivo* using His-GFP as a chromosome marker. These phenotypes include increased spacing between chromosomes and variability in DNA content and nuclear size. **f**, In nuclei showing a dramatic increase of the relative extrachromosomal volume, wider gaps between chromosomes are correlated with an enlargement of the EAST-labelled domain (red). This phenotype is reminiscent of the heat-shock-induced alteration of nuclear structure (see Fig. 3d). **g**, Abnormally expanded extrachromosomal nuclear territories between chromosomes and along the periphery of chromosomes (arrow) show co-localization of EAST (red) and CP60 (green), with zones of overlap appearing yellow in the merged image. **h**, A gap between chromosomes and the nuclear envelope labelled by anti-lamin shows continuous EAST staining (arrow). Scale bars represent 200 μm (**a,b**); 10 μm (**c–h**).

results in raised levels of nuclear EAST and increased spacing between chromosomes. The coincidence of these events suggests at least two alternative explanations. Heat shock could lead to an increase of EAST which, in turn, causes an expansion of the END; alternatively, heat shock could produce an inflation of the END, to which EAST is recruited in a secondary event. To distinguish between these two possibilities, full-length *east* cDNA was overexpressed in salivary glands in the absence of heat shock using the GAL4 system[28]. *hs–GAL4* served as a strong salivary gland-specific driver and *ftz–GAL4* as a weak one. *hs–GAL4* (at 20 °C without heat shock) in combination with *UAS–east* (*hs–GAL4 > UAS–east* caused a massive increase of anti-EAST immunofluorescence in salivary glands whereas the combination of *ftz-GAL4* and *UAS–east* (*ftz–GAL4 > UAS–east*) resulted in a moderate increase in a subset of the nuclei. The two drivers also differed in their effects on the growth of the salivary glands. *hs–GAL4 > UAS–east* leads to a dramatic reduction of the length and diameter of third-instar salivary glands compared with wild-type control larvae raised under identical conditions (Fig. 4a, b). In contrast, *ftz–GAL4 > UAS–east* did not affect the growth of salivary glands (data not shown). Overexpression of *east* in salivary glands did not affect viability or fertility.

Overexpression of *east* using the *hs–GAL4* driver resulted in high variability among polytene nuclei with respect to DNA content (area and intensity of DNA staining), diameter of the nuclear envelope and configuration of chromosomes (Fig. 4c, d). The transgenically expressed EAST protein was targeted to the correct nuclear compartment as it remained excluded from the chromosomal and nucleolar territories (Fig. 4f–h). Compared with control wild-type larvae raised at the same temperature, the relative nuclear volume occupied by the END increased and that of the chromosomes decreased. The majority of the nuclei in *hs–GAL4 > UAS–east* larvae had a wider spacing between chromosome strands in combination with an expansion of the END between those chromosome strands. Increased spacing between chromosomes and the variability of nuclear morphology could also be observed *in vivo* using histone–GFP as a marker for DNA in the same genetic background (Fig. 4e). Hence, transgenic overexpression of *east* under non-heat-shock conditions (for example 20 °C as shown here) can produce similar alterations in nuclear architecture to those induced by heat shock (compare Figs 3d and Fig. 4f). As in the heat-shock scenario, EAST in the enlarged extrachromosomal space showed co-localization with CP60 (Fig. 4g). Control wild-type larvae and transgenic larvae carrying only one of the transgenes, both raised without heat shock, did not show any of these nuclear alterations.

These results suggested the idea that increased levels of EAST might promote the expansion of an extrachromosomal nuclear domain, thereby positively modulating nuclear volume (compare the model in Fig. 8). However, because nuclear volume also depends on DNA content, and strong *east* overexpression resulted in a variable repression of endoreplication (Fig. 4b, d), nuclei containing raised levels of EAST did not necessarily have larger volumes than nuclei in wild-type salivary glands. Weaker *east* overexpression driven by *ftz–GAL4* resulted in an increased spacing between chromosomes in only a small proportion of nuclei. No dramatic inhibition of endoreplication was observed, however, thus allowing a direct comparison of nuclear volume and amount of EAST in nuclei containing about the same amount of DNA (Fig. 5). For adjacent nuclei showing a different spacing between chromosomes, the integrated levels of anti-EAST immunofluorescence and the corresponding nuclear areas in different focal planes were measured. The DNA content was quantified by measuring the level of fluorescence produced by histone–GFP. The measurements revealed a positive

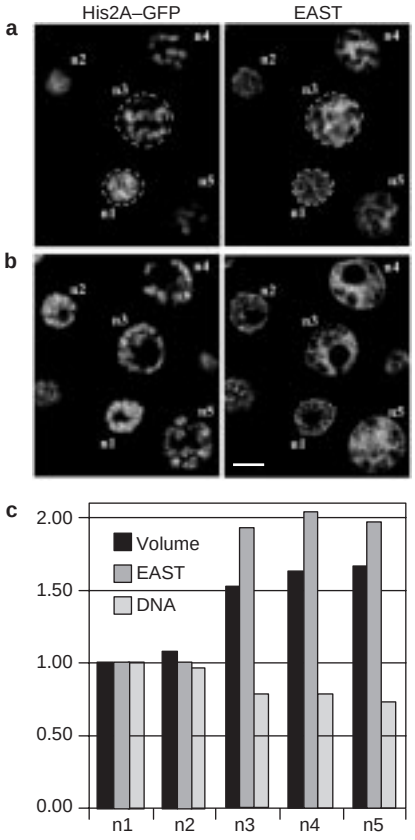

Figure 5 **Correlation of EAST protein and nuclear volume.** The overexpression of *east* in salivary glands of *ftz–GAL4 > UAS–east; His–GFP* can lead to an expansion of extrachromosomal regions in a subset of the nuclei. (**a, b**) The increased spacing between chromosomes in nuclei n3–n5 is associated with an increased nuclear volume compared with n1–n2, where chromosomes show a more compressed distribution. The focal planes of the sections in (**a**) and (**b**) are 2.5 μm apart. (**c**) Anti-EAST immunofluorescence is positively correlated with nuclear volume, whereas volume and DNA staining do not show any correlation. For instance, the largest nucleus, n5, has 66% more lumen and 97% more EAST than the smallest nucleus, n1. However, its total DNA signals are around 20% less. Bars represent the relative values of nuclear volume, histone–GFP fluorescence and anti-EAST fluorescence. The values corresponding to the smallest nucleus (n1) with an estimated lumen of 1,156 μm^3 were used as a standard of 1 for comparison. Images of anti-EAST staining and histone-GFP fluorescence were recorded for different focal planes that were 0.5 μm apart, with the heights along the *z*-axis of the nuclei displayed ranging from 9.5 to 11.0 μm. Lines were drawn along the boundaries of anti-EAST staining (example in **a**). The pixels within the boundaries were counted and the integrated signal intensities of anti-EAST and histone–GFP fluorescence were measured. The total values were sums of the values for each focal plane. Scale bar (**b**) represents 10 μm.

correlation between the quantity of EAST and nuclear volume (Fig. 5c). DNA signals in larger nuclei were comparable to or even slightly lower than those in smaller ones. Chromosomes in larger nuclei were also more widely spaced (this is most obvious near the nuclear periphery, Fig. 5a), further strengthening the notion that increased amounts of EAST can drive the expansion of an extrachromosomal domain, leading to an increase of nuclear volume.

Strong persistent transgenic *east* overexpression by *hs–GAL4* elicited effects which were not seen under low levels of transgenic east overexpression or in wild-type larvae exposed to heat shock. Whereas all three paradigms could result in an expansion of the END between chromosomes, only strong persistent overexpression could cause the END to extend peripherally beyond the zone occupied by the polytene chromosomes. This resulted in a marked gap between chromosomes and the nuclear envelope (Fig. 4d, n3) that showed anti-EAST labelling (Fig. 4h). EAST and CP60 also co-localized in this zone from the periphery of the chromosome mass to the nuclear envelope (Fig. 4g). In summary, excessive production of EAST drives the assembly of an enlarged extrachromosomal structure between chromosome strands or between the chromosome mass and the nuclear envelope that is able to recruit CP60.

EAST modulates nuclear actin. Two considerations prompted us to investigate a possible link between EAST and the regulation of nuclear actin. First, there is a striking resemblance in the interchromosomal network-like distribution patterns of EAST in polytene nuclei of *Drosophila* and actin in interphase nuclei of dinoflagellates[14]; second, many cellular rearrangements and movements are mediated by the actin cytoskeleton. To address this question, wild-type larvae and transgenic larvae overexpressing EAST were labelled by immunofluorescence using an anti-actin antibody. We used a commercial antibody that labels all of the structures known to be enriched for actin cytoskeleton (for example, cell cortex, cleavage furrows during cytokinesis, axon tracts; data not shown). In nuclei of wild-type salivary glands (Fig. 6a) and in tissues of transgenic larvae where EAST was expressed at normal levels (such as the proventriculus in Fig. 6c), anti-actin staining was either weak or undetectable. Anti-actin immunofluorescence in the cytoplasm was as strong as or stronger than in the nucleus. The detectable nuclear anti-actin immunofluorescence was diffusely distributed in the nucleoplasm and excluded from the nucleolus (Fig. 6d, arrowhead). Compared with wild type, anti-actin immunofluorescence was greatly increased in nuclei of salivary glands overexpressing EAST, with signal intensities generally higher than those seen in the cytoplasm (Fig. 6b, c). Nuclear actin staining was enriched in the extrachromosomal space, except the nucleolus, displaying extensive co-localization with EAST (Fig. 6e). To test if the increased anti-actin labelling was due to formation of filamentous actin, double labellings with anti-actin and phalloidin were performed. None of the nuclei showing anti-actin labelling was stained by phalloidin, however, suggesting that the bulk of nuclear actin is either not filamentous or forms filaments that do not interact with phalloidin (Fig. 6f). The enhanced anti-actin signals in response to overexpression of EAST and the co-localization of EAST and nuclear actin suggest that EAST might be regulating nuclear actin (see Discussion).

Effects of EAST overexpression on diploid cells. So far, our conclusions have been solely derived from studies on polytene tissues. The germline-specific driver *nanos–GAL4–VP16* (ref. 29) in combination with *UAS–east* (*nanos–GAL4 > UAS–east*) was used to overexpress EAST in diploid germline cells. A substantial increase in anti-EAST immunofluorescence was observed in a subset of cells near the tip of testes of late pupal and adult males (Fig. 7b). The cells showing increased anti-EAST signals in the nucleus were identified as germline stem cells and spermatogonia. The activation of *nanos–GAL4–VP16* in these germline cells but not in somatic cells or spermatocytes was confirmed using a *UAS–tau–GFP*[30] reporter gene (Fig. 7a). Germline stem cells contact the somatic hub cells at the tip of the testis and divide radially to give rise to a stem cell which remains in contact with the hub cells and a primary spermatogonium which is displaced away from the hub[31,32]. The primary spermatogonium then undergoes four incomplete divisions to produce a cyst of 16 secondary spermatogonia which remain connected via cytoplasmic bridges and will later differentiate into spermatocytes. Overexpression of EAST in these diploid germ cells did not cause male infertility. However, higher levels of EAST were associated with a distribution of the signals over larger regions of the nucleus (Fig. 7c–f), with the highest signal intensities being located along the nuclear periphery (Fig. 7f). As in the case of salivary glands, high levels of *east* overexpression could result in the formation of an EAST-labelled zone separating the bulk of the centrally located chromatin from the nuclear envelope (Fig. 7f). By contrast, germline cells of control animals showed a more even distribution of

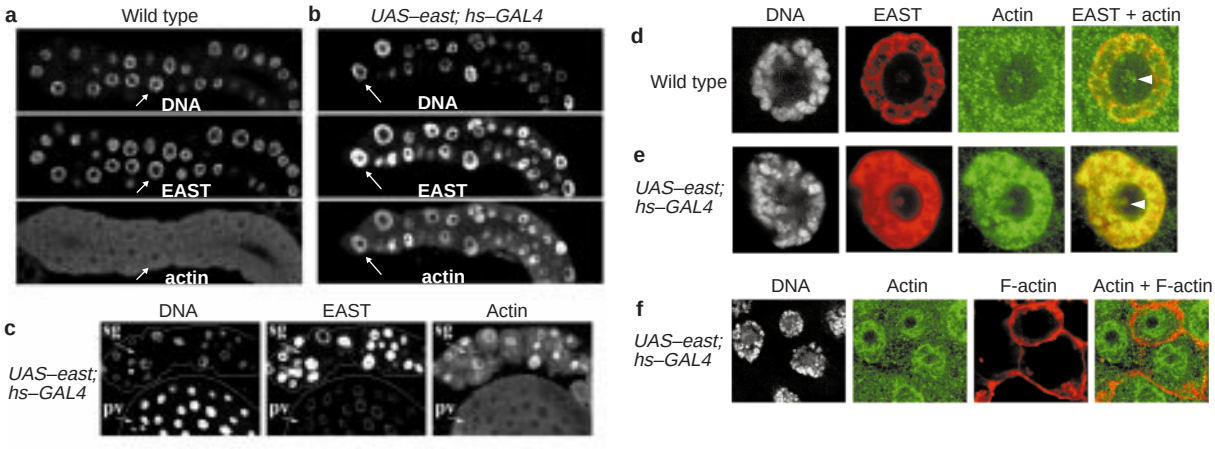

Figure 6 **EAST modulates the levels of nuclear actin.** Salivary glands of feeding wild-type (**a, d**) and transgenic *UAS–east*; *hs–GAL4* (**b, c, e**) third-instar larvae were stained using DNA stain, anti-EAST and anti-actin. In the close-ups of single nuclei (**d, e**), which are indicated by arrows in (**a, b**) EAST is red and actin green. Areas of co-localization appear yellow. In the wild type (**a, d**), anti-actin immunofluorescence is of similar intensity in cytoplasm and nuclei. Overexpression of EAST (**b, e**) leads to a dramatic increase of nuclear actin labelling, which shows a higher intensity relative to the cytoplasmic actin signal. Both EAST and actin are extensively co-localized within the nucleus and are excluded from the nucleolus (arrowheads). **c**, In contrast to salivary glands (sg), a distinct nuclear anti-actin staining cannot be detected in the proventriculus (pv) or other tissues of transgenic animals, which show normal levels of EAST. **f**, Nuclei of transgenic salivary glands showing anti-actin signals (green) are not co-labelled by phalloidin (red).

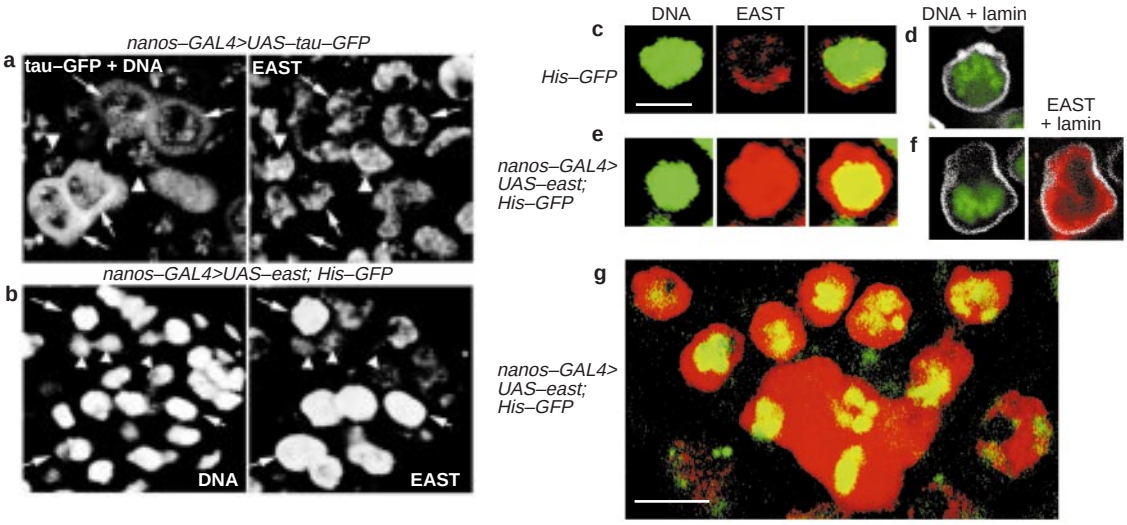

Figure 7 **Overexpression of EAST in diploid cells can expand extrachromosomal structures.** *UAS–east* expression driven by *nanos–GAL4–VP16* results in a drastic increase of EAST in nuclei of germline stem cells and spermatogonia. **a**, EAST expression in a testis of a *nanos–GAL4 > UAS–tau–GFP* control animal. The cytoplasmic tau–GFP reporter labels cysts of spermatogonia. Little variation in EAST labelling is seen between the spermatogonia labelled with tau– (arrows) and somatic cyst cells, which are not labelled (arrowheads). SPIF was used for the visualization of DNA. **b**, Greatly increased EAST levels were detected in germ cells (arrows) compared with somatic cells (arrowheads) of *nanos–GAL4 > UAS–east*; *His–GFP* males. Strong labelling is found in germline stem cells adjacent to a cluster of somatic hub cells (marked with an asterisk) and in more distal spermatogonia. The drastic increase of nuclear EAST (red) in *nanos–GAL4 > UAS–east* (**e, f**) compared with control (**c**) germ cells is associated with the formation of a distinct gap between a central chromatin mass (green) and the nuclear envelope (white). In germ cells of *His–GFP* controls (**c, d**), chromatin is more evenly distributed in the nuclear lumen. **f**, Overexpressed EAST protein preferentially accumulates in a peripheral region of the nuclear lumen along the inside of the lamina. Note that the rabbit anti-EAST antibody used for double labelling with mouse anti-lamin (**d, f**) is less sensitive than the mouse anti-EAST antibody used in (**c, e**) and unable to detect EAST in wild-type testes. **g**, The extrachromosomal nuclear domains of different EAST-overexpressing spermatogonia sometimes show fusion. The condensed chromatin masses (green) characteristic of spermatogonia are separated whereas EAST-labelled regions (red) are fused. Scale bar in g represents 10 μm and also refers to **a** and **b**; scale bar in **c** represents 5 μm and also refers to **c–f**.

chromatin throughout the nuclear lumen, without the formation of a distinct gap between the chromatin mass and the nuclear envelope (Fig. 7d).

To test if the overproduction of EAST might lead to an increase of nuclear volume of diploid cells, z-sections (sections along the *z*-axis) of anti-lamin-labelled testes of *nanos–GAL4 > UAS–east* and *nanos–GAL4 > UAS–tau–GFP* males were used to determine nuclear volumes of germline stem cells. Germline stem cells were identified on the basis of their position adjacent to hub cells and expression of either high levels of EAST, for *nanos–GAL4 > UAS–*

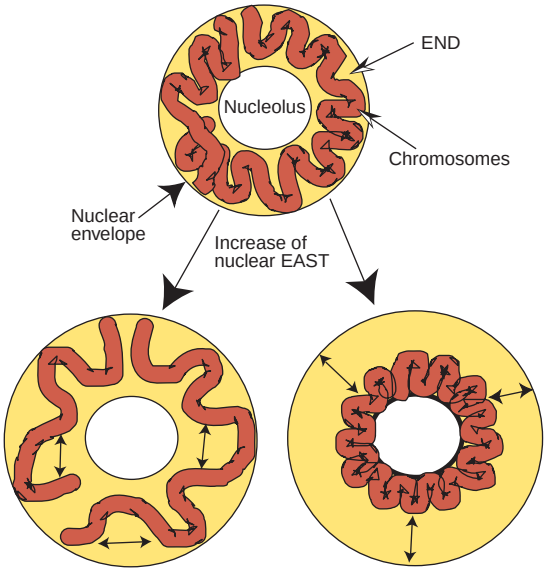

Figure 8 **Proposed mechanism for the involvement of EAST in shaping nuclear architecture.** The accumulation of EAST within the nucleus causes an enlargement of the END (yellow). The force generated by the expansion of this putative nuclear endoskeleton results in context-dependent chromosome rearrangements. Chromosomes (red) can either increase their spacing, if the END expands mainly between chromosomes (left), or be compressed to a smaller volume if the enlargement of the END mainly occurs between chromosomes and nuclear membrane (right).

east, or cytoplasmic tau-GFP for *nanos–GAL4 > UAS–tau–GFP* controls. The largest nuclei of the *east*-overexpressing stem cells (up to 72 μm^3 in volume) showed approximately 20% more lumen than the largest nucleus found in the control testes (60 μm^3), suggesting that the expansion of an extrachromosomal domain might also result in a slightly increased size of diploid nuclei. The expansion of extrachromosomal regions could occasionally reach even more extreme proportions in spermatogonia. We observed continuous EAST-labelled territories containing more than one chromatin mass of normal size (Fig. 7g), suggesting that daughter nuclei, following segregation during mitosis, might have been engulfed by a giant shared extrachromosomal domain. The overabundance of EAST during reassembly of the interphase nucleus after mitosis could produce extended extrachromosomal structures. Because cytokinesis of spermatogonia is incomplete, the enlarged extrachromosomal structures forming around the two separate daughter nuclei might become linked via cytoplasmic bridges.

Discussion

Our data support the existence of a meshwork-like nuclear endoskeleton localized to the extrachromosomal space. EAST labels and defines the END, an extrachromosomal nuclear domain that pervades the interior of polytene nuclei and lines the inner side of the nuclear envelope and the outer side of the nucleolus (Fig. 8). The END appears as a dynamic and flexible structure as it can increase its volume in response to a higher dosage of *east*. This swelling of the END results in a widening of the gaps between chromosome strands, suggesting a role for this structure in the global arrangement of chromosomes. EAST appears to be one of the factors involved in modulating the relative volume of the END in diploid and polyploid nuclei. This idea is supported by the observation that transgenic overexpression of *east* can result in the dramatic expansion of extrachromosomal regions between chromosomes or between chromosomes and the nuclear envelope.

Our data favour a model in which EAST fuels the assembly and expansion of a nuclear endoskeleton that can recruit other nuclear proteins. One of these proteins is CP60; in interphase nuclei of embryos, CP60 has been shown to be distributed in a fibrous pattern, which does not overlap with DNA, suggesting that it could be part of a nucleoskeleton[27]. Consistent with the potential role of EAST in the assembly, maintenance or alteration of an extrachromosomal nucleoskeleton, we demonstrate not only that CP60 largely co-localizes with EAST, but that its extrachromosomal localization also depends on *east* function. In the absence of EAST, this structural backbone fails to assemble correctly, resulting in the abnormal localization of CP60 inside the nucleus. On the other hand, when EAST production is artificially enhanced, this hypothetical nuclear endoskeleton is enlarged, resulting in CP60 being recruited to greatly expanded extrachromosomal territories within the nucleus (Fig. 4g). Our results raise the intriguing possibility that actin may be another component that is recruited to the nucleoskeleton formed under the influence of EAST. Previous studies have suggested that the immunocytochemical detection of actin in the nucleus might be difficult because it mostly occurs in a monomeric and soluble form that is readily extracted by detergents[15]. We failed to detect filamentous actin using phalloidin, suggesting that the massive increase of nuclear anti-actin immunofluorescence under the influence of EAST overproduction might not result from an increase in actin polymerization. Instead, we favour a scenario in which increased formation of nucleoskeletal structures leads to a higher binding capacity for actin monomers, rendering them resistant to solubilization by detergent. Taken together, these observations suggest that EAST is instrumental in defining the extent of an extrachromosomal nuclear structure that provides anchorage for other molecules like CP60 and actin.

EAST is a novel protein without functional domains identified in other proteins. Two conceivable mechanisms can explain how increased levels of EAST might lead to an expansion of the END. EAST might serve as a structural building block that becomes incorporated into a scaffold structure. Alternatively, EAST might catalyse the formation of a nucleoskeleton by regulating one of its building blocks. We cannot distinguish between these two possibilities. The high number of potential PEST sequences within the EAST protein suggests a tight regulation of its activity. Rapid destruction of EAST mediated by the PEST regions would enable the dynamic disassembly of a putative nucleoskeleton. The need to keep EAST activity in check is highlighted by the dramatic effects on nuclear structure caused by persistent transgenic overexpression of EAST in salivary glands. Moreover, ubiquitous overexpression of this transgene in embryos results in complete embryonic lethality (M.W. and W.C., unpublished results). The relevance of EAST-mediated chromosome rearrangements remains a matter of speculation. The activation of EAST during heat shock could strengthen the END, thereby preventing the collision of neighbouring chromosome arms. Interestingly, lamin B, another structural protein of the nucleus, also shows increased synthesis in response to hyperthermia[33]. The inflation of the extrachromosomal space may influence gene expression, as RNA transport has been shown to occur in this compartment[17].

In this study we mainly focused on polyploid and non-dividing cells. EAST is, however, also expressed in dividing diploid cells. Levels of EAST protein are cell cycle dependent in proliferating cells and *east* mutations affect both mitotic and meiotic divisions (M.W. and W.C., unpublished results). Hence the role of *east* in modulating nuclear architecture, which we have illustrated here using the larval polytene nuclei as a model, is likely to be relevant to the alterations of chromosomal organization during the cell cycle of diploid tissues. □

Methods

Fly stocks

The isolation of the viable P-element insertion $east^{P[ETX3]}$ has been previously described[21]. The lethal alleles $east^{hop\text{-}4}$ and $east^{hop\text{-}7}$ were generated by imprecise excision of the P element in $east^{P[ETX3]}$ (ref. 21). X-

chromosomes carrying lethal *east* alleles were balanced with FM7c-blue. Canton-S was used as the wild-type strain. The GAL4 driver *hs–GAL4*^{M4} (provided by J. Roote) drives high levels and *ftz–GAL4* (provided by C. Doe) low levels of salivary gland expression even at low temperature (e.g. 20 °C), presumably owing to the presence of a salivary-gland-specific enhancer in the GAL4 driver constructs. The line carrying a *His2AvDGFP* fusion gene[25] was obtained from R. Saint, the line carrying *UAS–tau–GFP* from A. Brand, and the line carrying *nanos–GAL4–VP16* from the Bloomington Stock Center.

Cloning of *east*

Flanking genomic DNA next to the insertion site of *east*$^{P[ETX3]}$ was isolated by plasmid rescue and used to screen a genomic library[34]. Clones comprising about 26 kb of genomic DNA surrounding the insertion site were isolated. Because a previously isolated 1.0 kb cDNA clone which lacked any open reading frame (ORF)[21] hybridized to the *east* genomic DNA, it was used to screen an embryonic cDNA library for larger clones[35]. Polyadenylated RNA extracted from adult flies served as the template for 5′ RACE.

Generation of anti-EAST antibodies

Four different regions of EAST were expressed with an N-terminal hexa-histidine tag (His_6) using the QIAexpress system from Qiagen. The four different cDNA regions (ED1, amino acids 255–469; ED2, 715–822; ED3, 823–986; ED4, 1483–1850) were amplified by PCR and fused in frame with the nucleotides encoding the His_6 tag in the expression vectors pQE30–pQE32. Bacterially produced fusion proteins were purified using Ni-NTA resin, which binds selectively to the His_6 tag. The purified fusion proteins were used to immunize Balb/c female mice. Fusion protein ED2 was also used to immunize a rabbit. Polyclonal mouse and rabbit anti-EAST sera were obtained after five injections.

Immunocytochemistry and confocal microscopy

Larvae were raised at 20 °C on yeast glucose medium (unless otherwise stated) and dissected in Ringer's medium[36]. Third-instar larvae were collected between 10–11 days after egg laying. Heat shock was applied for 1 h in an air incubator set to 37 °C. The heat-shock response observed in salivary glands was most pronounced in early feeding third-instar larvae with smaller nuclei, whereas the older wandering larvae with larger nuclei did not show increased EAST levels and altered chromosome arrangements. Larval tissues were fixed in 4% paraformaldehyde in PBS for 15 min, washed in PBT (PBS, 0.1% Triton-X-100) and blocked in PBT, 1% BSA for 1 h. Samples were incubated in anti-EAST at a 1:1000 dilution in PBT, 1% BSA overnight at 4 °C. The polyclonal rabbit anti-CP60 (ref. 37) and monoclonal mouse anti-lamin Dm0 (ref. 38) antibodies have been previously described. Anti-actin staining was performed using a commercial affinity-purified polyclonal rabbit anti-actin antibody (Sigma) at 1:100 dilution. Secondary immunofluorescence detection was carried out using Cy3- or Cy5-coupled goat anti-mouse or goat anti-rabbit antibodies (Immuno Jackson) at the recommended dilution in PBT, 1% BSA for 2 h at room temperature. Filamentous actin was labelled using phalloidin-TRITC (Sigma). After washing, the samples were mounted in SPIF for the visualization of DNA[39]. When His2AvDGFP was used as a marker for chromosomes in fixed tissues, the samples were mounted in Vectastain. For *in vivo* observations using histone–GFP, larval tissues were dissected in Ringer's solution and transferred to Schneider's culture medium on a microscope slide for analysis. Testes were dissected from late pupae and early adults and fixed and stained like larval tissues. Images of fluorescently labelled tissues were acquired on a Bio-Rad MRC 1024 confocal microscope. Digital images were processed using Confocal Assistant 4.02 and Adobe Photoshop 4.0 software. The approximate volume of nuclei in salivary glands and testes was calculated from confocal z-sections recorded at intervals of 0.5 µm. Using the marquee function in Photoshop, a line was drawn around the boundary of the nuclear area (Fig. 5a). The area was measured using the histogram function. The volume was derived from adding up the volumes of all 0.5 µm thick sections corresponding to an individual nucleus.

Overexpression of *east* using the GAL4 system

The *UAS–east* transgene was constructed by inserting a *Not*I–*Nhe*I fragment containing the entire ORF of the *east* cDNA into the *Not*I–*Xba*I sites of the pUAST vector[28]. Transgenic flies were generated using standard P-element-mediated transformation techniques[40]. To overexpress *east*, males carrying the homozygous transgene *UAS–east* on the second chromosome were crossed to virgin females carrying various GAL4 driver constructs. The homozygous heat-shock-inducible *hs–GAL4*^{M4} transgene on the third chromosome was found to be expressed in a heat-shock-independent fashion in larval salivary glands, as drastically increased levels of EAST were detected at temperatures as low as 17 °C. The *ftz–GAL4* driver on the third chromosome was used for low levels of *UAS–east* expression in salivary glands. The *nanos–GAL4–VP16* (ref. 29) driver was used to direct *UAS–east* expression in germline stem cells and spermatogonia of testes.

RECEIVED 20 OCTOBER 1999; REVISED 4 FEBRUARY 2000; ACCEPTED 17 MARCH 2000; PUBLISHED 4 APRIL 2000.

1. Cremer, T. *et al.* Role of chromosome territories in the functional compartmentalization of the cell nucleus. *Cold Spring Harb. Symp. Quant. Biol.* **58,** 777–792 (1993).
2. Marshall, W. F., Fung, J. C. & Sedat, J. W. Deconstructing the nucleus: global architecture from local interactions. *Curr. Opin. Genet. Dev.* **7,** 259–263 (1997).
3. van Driel, R. *et al.* Nuclear domains and the nuclear matrix. *Int. Rev. Cytol.* **162A,** 151–189 (1995).
4. Jackson, D. A. Chromatin domains and nuclear compartments: establishing sites of gene expression in eukaryotic nuclei. *Mol. Biol. Rep.* **24,** 209–220 (1997).
5. Spector, D. L. Nuclear organization and gene expression. *Exp. Cell Res.* **229,** 189–197 (1996).
6. Wei, X. *et al.* Segregation of transcription and replication sites into higher order domain. *Science* **281,** 1502–1506 (1998).
7. Abney, J. R., Cutler, B., Fillbach, M. L., Axelrod, D. & Scalettar, B. A. Chromatin dynamics in interphase nuclei and its implications for nuclear structure. *J. Cell Biol.* **137,** 1459–1468 (1997).
8. Marshall, W. F. *et al.* Interphase chromosomes undergo constrained diffusional motion in living cells. *Curr. Biol.* **7,** 930–939 (1997).
9. Chu, A., Rassadi, R. & Stochaj, U. Velcro in the nuclear envelope: LBR and LAPs. *FEBS Lett.* **441,** 165–169 (1998).
10. Stuurman, N., Heins, S. & Aebi, U. Nuclear lamins: their structure, assembly, and interactions. *J. Struct. Biol.* **122,** 42–66 (1998).
11. Berezney, R. & Coffey, D. S. Identification of a nuclear protein matrix. *Biochem. Biophys. Res. Commun.* **60,** 1410–1417 (1974).
12. Pederson, T. Thinking about a nuclear matrix. *J. Mol. Biol.* **277,** 147–159 (1998).
13. Nakayasu, H. & Ueda, K. Association of actin with the nuclear matrix from bovine lymphocytes. *Exp. Cell Res.* **143,** 55–62 (1983).
14. Soyer-Gobillard, M. O., Ausseil, J. & Geraud, M. L. Nuclear and cytoplasmic actin in dinoflagellates. *Biol. Cell* **87,** 17–35 (1996).
15. Nguyen, E., Besombes, D. & Debey, P. Immunofluorescent localization of actin in relation to transcription sites in mouse pronuclei. *Mol. Reprod. Dev.* **50,** 263–272 (1998).
16. Zirbel, R. M., Mathieu, U. R., Kurz, A., Cremer, T. & Lichter, P. Evidence for a nuclear compartment of transcription and splicing located at chromosome domain boundaries. *Chromosome Res.* **1,** 93–106 (1993).
17. Zachar, Z., Kramer, J., Mims, I. P. & Bingham, P. M. Evidence for channeled diffusion of pre-mRNAs during nuclear RNA transport in metazoans. *J. Cell Biol.* **121,** 729–742 (1993).
18. Zimowska, G., Aris, J. P. & Paddy, M. R. A Drosophila Tpr protein homolog is localized both in the extrachromosomal channel network and to nuclear pore complexes. *J. Cell Sci.* **110,** 927–944 (1997).
19. Bridger, J. M., Herrmann, H., Munkel, C. & Lichter, P. Identification of an interchromosomal compartment by polymerization of nuclear-targeted vimentin. *J. Cell Sci.* **111,** 1241–1253 (1998).
20. Anand, A. *et al. Drosophila* "enhancer-trap" transposants: Gene expression in chemosensory and motor pathways and identification of mutants affected in smell and taste ability. *J. Genet.* **69,** 151–168 (1990).
21. VijayRaghavan, K., Kaur, J., Paranjape, J. & Rodrigues, V. The east gene of Drosophila melanogaster is expressed in the developing embryonic nervous system and is required for normal olfactory and gustatory responses of the adult. *Dev. Biol.* **154,** 23–36 (1992).
22. Nakai, K. & Horton, P. PSORT: a program for detecting the sorting signals of proteins and predicting their subcellular localization. *Trends Biochem. Sci.* **24,** 34–35 (1999).
23. Rechsteiner, M. & Rogers, S. W. PEST sequences and regulation by proteolysis. *Trends Biochem. Sci.* **21,** 267–271 (1996).
24. Agard, D. A. & Sedat, J. W. Three-dimensional architecture of a polytene nucleus. *Nature* **302,** 676–681 (1983).
25. Clarkson, M. & Saint, R. A His2AvDGFP fusion gene complements a lethal His2AvD mutant allele and provides an in vivo marker for Drosophila chromosome behavior. *DNA Cell Biol.* **18,** 457–462 (1999).
26. Kellogg, D. R., Oegema, K., Raff, J., Schneider, K. & Alberts, B. M. CP60: a microtubule-associated protein that is localized to the centrosome in a cell cycle-specific manner. *Mol. Biol. Cell* **6,** 1673–1684 (1995).
27. Oegema, K., Marshall, W. F., Sedat, J. W. & Alberts, B. M. Two proteins that cycle asynchronously between centrosomes and nuclear structures: Drosophila CP60 and CP190. *J. Cell Sci.* **110,** 1573–1583 (1997).
28. Brand, A. H. & Perrimon, N. Targeted gene expression as a means of altering cell fates and generating dominant phenotypes. *Development* **118,** 401–415 (1993).
29. Van Doren, M., Williamson, A. L. & Lehmann, R. Regulation of zygotic gene expression in Drosophila primordial germ cells. *Curr. Biol.* **8,** 243–246 (1998).
30. Brand, A. H. & Dormand, E. L. The GAL4 system as a tool for unravelling the mysteries of the Drosophila nervous system. *Curr. Opin. Neurobiol.* **5,** 572–578 (1995).
31. Gonczy, P. & DiNardo, S. The germ line regulates somatic cyst cell proliferation and fate during Drosophila spermatogenesis. *Development* **122,** 2437–2447 (1996).
32. Fuller, M. T. in *The Development of* Drosophila melanogaster (eds Bate, M. & Martinez-Arias, A.) 71–147 (Cold Spring Harbor Laboratory Press, NY, 1993).
33. Dynlacht, J. R., Story, M. D., Zhu, W. G. & Danner, J. Lamin B is a prompt heat shock protein. *J. Cell. Physiol.* **178,** 28–34 (1999).
34. Tamkun, J. W. *et al.* brahma: a regulator of Drosophila homeotic genes structurally related to the yeast transcriptional activator SNF2/SWI2. *Cell* **68,** 561–572 (1992).
35. Brown, N. H. & Kafatos, F. C. Functional cDNA libraries from Drosophila embryos. *J. Mol. Biol.* **203,** 425–437 (1988).
36. Ashburner, M. *Drosophila: A Laboratory Handbook.* (Cold Spring Harbor Laboratory Press, NY, 1989).
37. Kellogg, D. R. & Alberts, B. M. Purification of a multiprotein complex containing centrosomal proteins from the Drosophila embryo by chromatography with low-affinity polyclonal antibodies. *Mol. Biol. Cell* **3,** 1–11 (1992).
38. Gruenbaum, Y. *et al.* Drosophila nuclear lamin precursor Dm0 is translated from either of two developmentally regulated mRNA species apparently encoded by a single gene [Erratum *J. Cell Biol.* **106,** 2225 (1988)]. J. Cell Biol. 106, 585–596 (1988).
39. Lundell, M. J. & Hirsh, J. A new visible light DNA fluorochrome for confocal microscopy. *Biotechniques* **16,** 434–440 (1994).
40. Spradling, A. in *Drosophila: A Practical Approach* (ed. Roberts, D. B.) 175-197 (IRL, Oxford, 1986).

ACKNOWLEDGEMENTS

We thank V. Rodrigues for discussion and comments on the manuscript, J. Kaur and V. Rodrigues for the east fly stocks prior to publication, G. Udolph for help with the germline transformation, A. Brand for the tau-GFP stock, J. Gruenbaum for anti-lamin, J. Raff for anti-CP60, R. Saint for the His2AvDGFP line and the Bloomington Stock Center for stocks. We thank the Institute of Molecular and Cell Biology for financial support.

Correspondence and requests for materials should be addressed to W.C. The Drosophila east cDNA sequence has been deposited in GenBank, accession number AF242291.

